https://doi.org/10.15302/frontphys.2025.055203

RESEARCH ARTICLE

# Near-room-temperature exchange bias in surface-oxidized $Fe_3GaTe_2$ revealed by reflective magnetic circular dichroism

Xinjie Li[1,2,*], Feiyue Wang[1,2,*], Chunyi Wu[1,2], Jialong Zhang[1,2], Guanqi Li[3,†], Jing Wu[3], Ya-Qing Bie[1,2,‡]

[1]State Key Lab of Optoelectronic Materials and Technologies, Guangdong Province Key Laboratory of Display Material and Technology, Sun Yat-sen University, Guangzhou 510006, China
[2] School of Electronics and Information Technology, Sun Yat-sen University, Guangzhou 510006, China
[3] School of Integrated Circuits, Guangdong University of Technology
[*]These authors contribute equally to this work.
Corresponding authors. E-mail: [†]lgq2010@gdut.edu.cn, [‡]bieyq@mail.sysu.edu.cn
Received January 14, 2025; accepted March 30, 2025

## Supporting Information

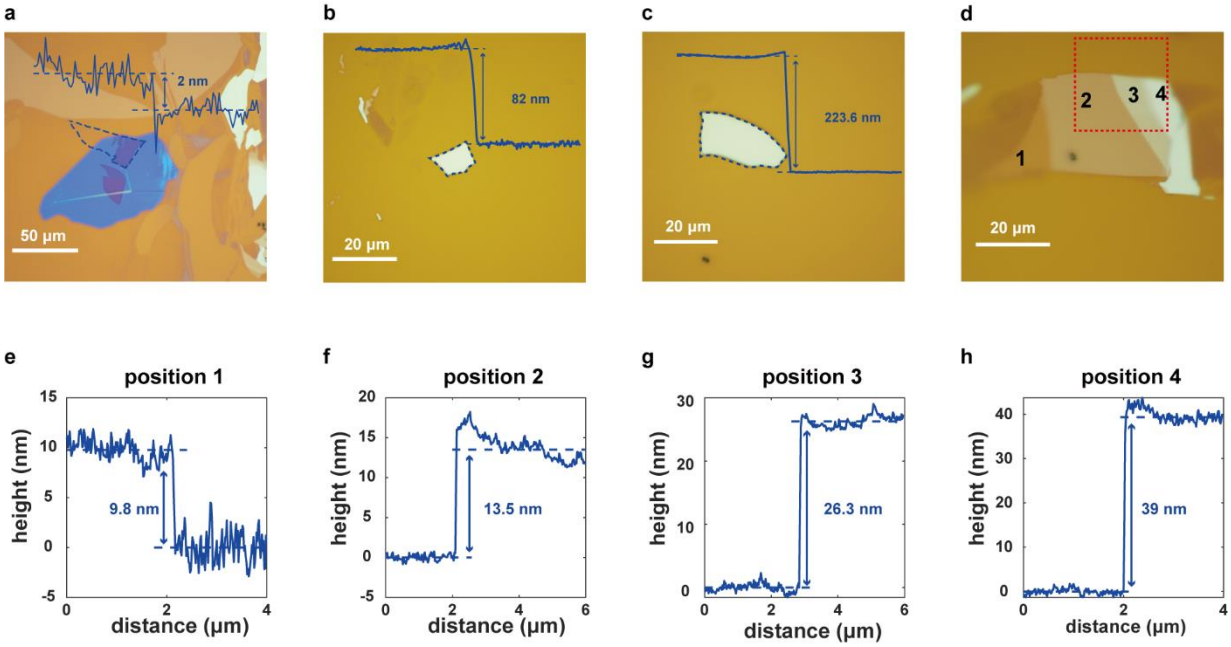


**Fig. S1 Optical images of flakes with different thickness.** The AFM are measured in air after the RMCD characterization. The dashed lines marked the flakes being studied. (a) A 2 nm and a 5 nm flake covered by an h-BN flake. The AFM was conducted near the edge of h-BN where the $Fe_3GaTe_2$ flake is only 2 nm. By comparing the optical contrast, we estimated that the red dashed line region is around 5 nm thick. (b) the 82 nm flake, (c) the 224 nm flake, and (d) the flake with multi-steps with thickness of (e) 9.8 nm, (f) 13.5 nm, (g) 26.3 nm and (h) 39 nm. These thicknesses are all confirmed with atomic force microscopy. The red dashed squares in (d) indicated the region for the RMCD mapping in Figure 4

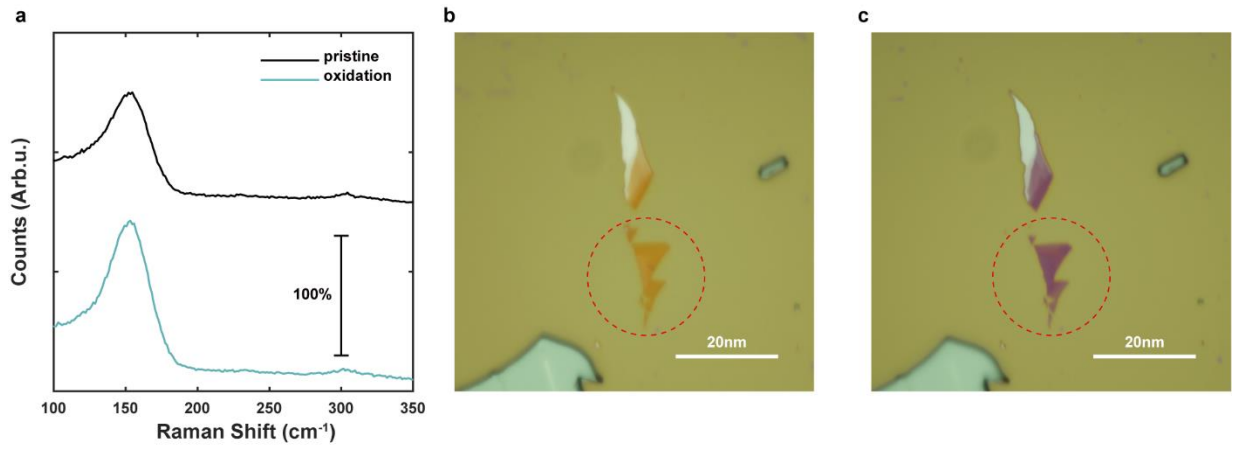


**Fig. S2 Raman spectroscopy of a thin $Fe_3GaTe_2$ flake exposed in air. The thickness was approximately 10 nm**. (a)The Raman spectra before and after exposing the material in air for 3 hrs. We did not observe significant difference in the spectra after the oxidation. (b, c) The optical image before and after the oxidation.

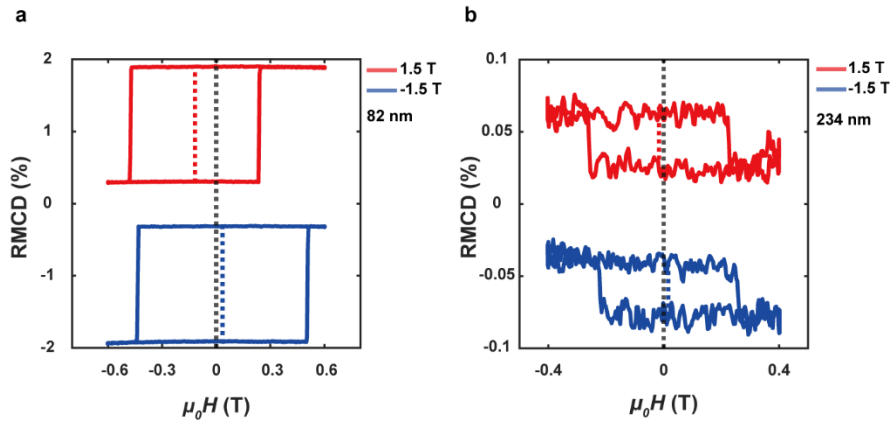


**Fig. S3 RMCD hysteresis loops of 82 nm, and 224 nm $Fe_3GaTe_2$ flakes at 40 K after spin polarization setting.** (a) Hysteresis loops of the 82 nm thick flake using 532 nm laser (b) Hysteresis loops of the 224 nm thick flake using 632.8 nm laser. The 632.8 nm laser has smaller RMCD signal but the coercive field and exchange bias is the same as that measured using 532 nm laser.

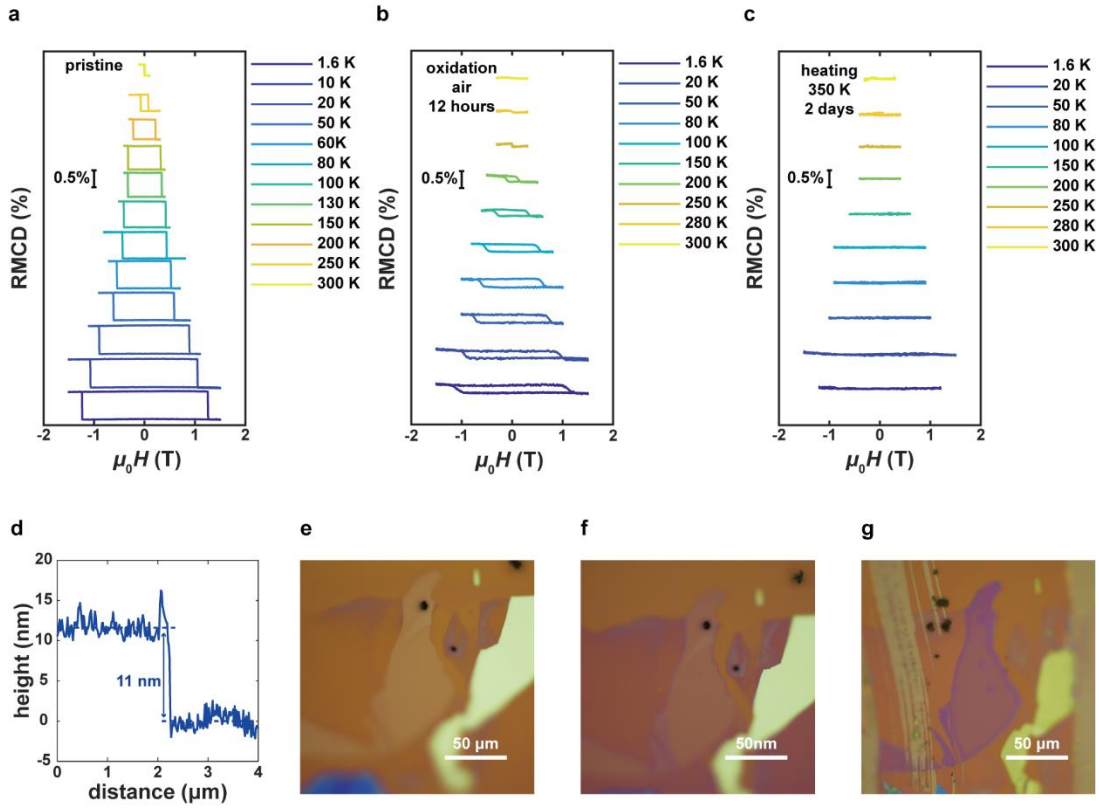


**Fig. S4** The RMCD loops of an 11 nm at different stages of oxidation and heating, measured at various temperatures without polarization setting. (a) Pristine state, (b)after 12 hours oxidation in air, and (c) after 350 K heating in air for 2 days. (d) Atomic force microscope characterization of the flake thickness (e, f, g) Optical images of the flake (e) pristine, (f) after 12 hrs oxidation in air and (g) after heating at 350 K in air for 2 days.

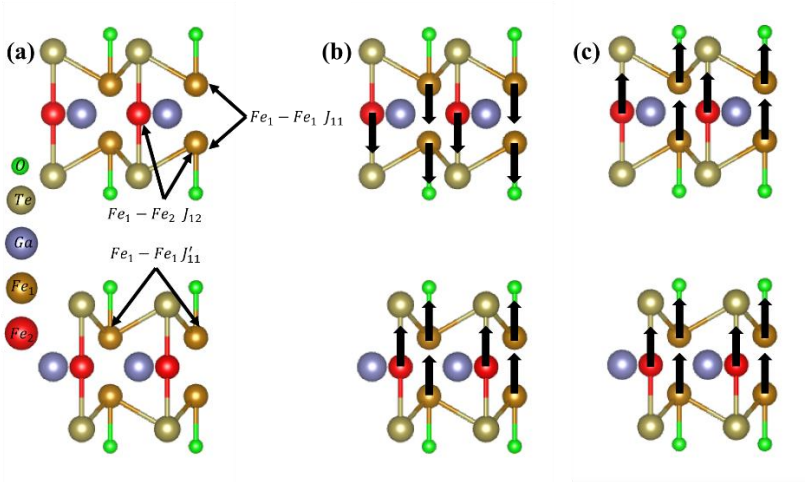


**Fig. S5** (a) Intralayer and interlayer exchange coupling between Fe atoms; Spin configurations implemented to calculate the system total energy for (b) interlayer antiferromagnetic coupling and (c) interlayer ferromagnetic coupling between the O-$Fe_3GaTe_2$ layers.

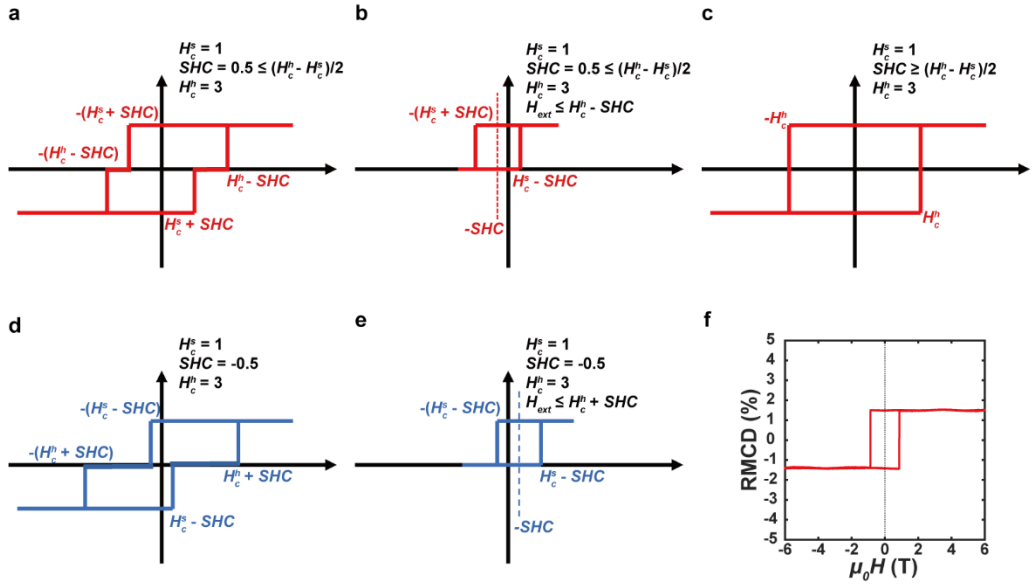


**Fig. S6 Full-field and minor field loops model for the soft and hard interlayer exchange coupling and the experimental result.** If the interlayer exchange coupling strength between the soft and hard layers (*SHC)* is ferromagnetic and $SHC \le (H_c^h - H_c^s)/2$, (a) symmetrical exchange bias will show in the full loop scan together with the double steps feature in each scan. (b) Minor loops scan with smaller field strength. In the minor loop scan, exchange bias is still visible, but spin flips of the soft layer occur at smaller field values. (c) If the interlayer coupling is too large $SHC \ge (H_c^h - H_c^s)/2$, no exchange bias will be observed. (d, e) For an antiferromagnetic interlayer exchange coupling $SHC = -(H_c^h - H_c^s)/2$, the full loop and the minor loop behaviors are illustrated as shown in (d, e) respectively. If we assume the pristine $Fe_3GaTe_2$ and the O-$Fe_3GaTe_2$ are ferromagnets and they are most likely ferromagnetically coupled, Figure 6a will be the model to explain the exchange bias between the soft and hard layer. (f) The RMCD loop of the 82 nm sample at 1.6 K with a full scan from ±6 T. The exchange bias disappears in the large field scan and no additional spin-flip steps appear. This excludes the possibility that the ±6 T flip the spins in hard layer (or antiferromagnets) to set the polarization direction.

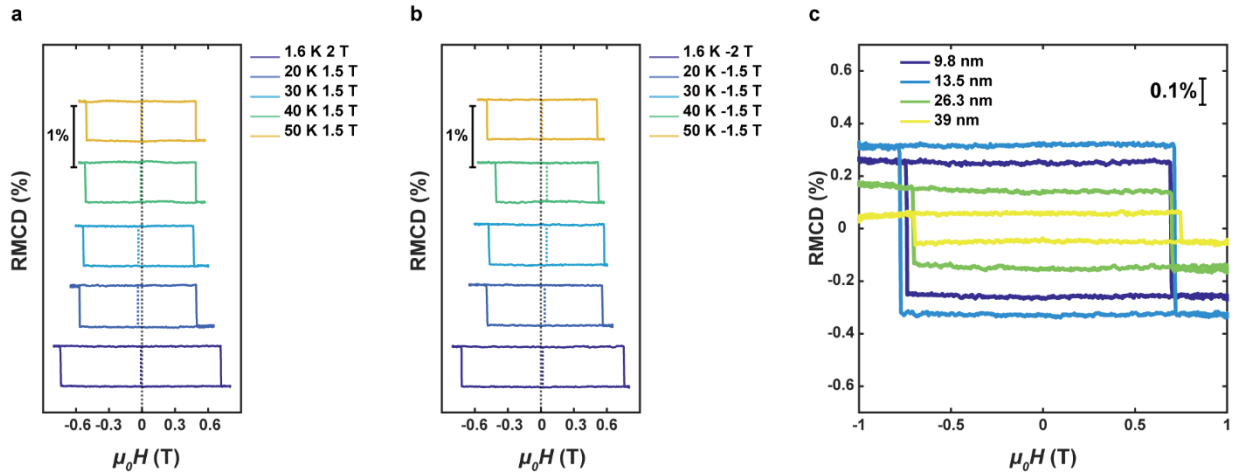


**Fig. S7** RMCD hysteresis loops of multi-step flakes with thicknesses of 9.8 nm, 13.5 nm, 26.3 nm, and 39 nm, measured using a 532 nm laser. (a) Hysteresis loops after applying a positive field and (b) after a negative field setting, measured at low temperatures from the 13.5 nm region. (c) Hysteresis loops measured at 1.6 K from the 9.8 nm, 13.5 nm, 26.3 nm, and 39 nm regions in sequence. The similarity of the loops suggests that spin flips occurred almost simultaneously across these regions.

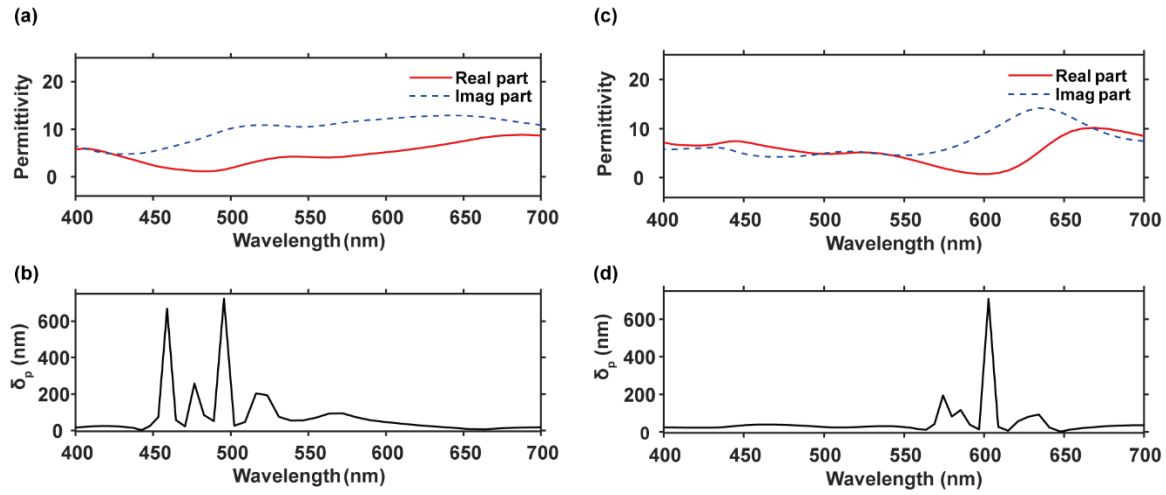


**Fig. S8** The calculated (a, c) dielectric constant and (b, d) the penetration depth of the O-$Fe_3GaTe_2$ and $Fe_3GaTe_2$ as a function of wavelength.

**Table S1** The calculated of interlayer exchange coupling energy and magnetic anisotropy energy (easy axis along [100] and [001] direction, respectively) $Fe_3GaTe_2$ (or partially oxidized $Fe_3GaTe_2$).

| Number of oxygen layers | Crystal structure | Spin antiparallel interlayer exchange energy (eV) | Spin parallel interlayer exchange energy (eV) | Energy difference (eV) | Magnetic anisotropy energy $E_{100} - E_{001}$ (eV) |
|---|---|---|---|---|---|
| 0 | 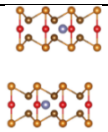 | -49.42008 | -49.50736 | 0.08728 | 0.04918 |
| 1 | 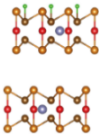 | -55.1335 | -55.16405 | 0.03054 | -0.28494 |
| 2 | 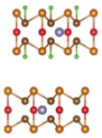 | -59.63218 | -59.94839 | 0.31621 | 0.00173 |
| 3 | 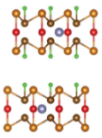 | -64.60348 | -64.70636 | 0.10288 | -0.11397 |
| 4 | 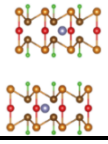 | -68.41629 | -68.19102 | -0.22527 | 0.01094 |

**Supplementary Note S1. $Fe_3GaTe_2$ flake preparation**

Most of the thin layer flakes were exfoliated on electronic-beam evaporated 2 nm/3 nm Ti/Au films on $SiO_2$/Si substrates inside an argon-filled glovebox, while the 5 nm flake was covered with h-BN to avoid oxidation. The h-BN was transferred on the $Fe_3GaTe_2$ sample using PDMS gel films with a transfer setup also inside the glovebox[1,2].

To prepare the sample for the STEM measurement, a platinum layer was deposited on the flake by the focus ion beam induced deposition. Then the sample was cut by gallium ion beam with the cross-section observable in the STEM measurement.

**Supplementary Note S2. The ab initio calculation of the interlayer coupling in $Fe_3GaTe_2$ and O-$Fe_3GaTe_2$**

Our computational approach utilized the Vienna ab initio simulation package (VASP) with the projector augmented wave (PAW) method to accurately describe electron-core interactions using the Perdew-Burke-Ernzerhof (PBE) functional framework[3-5]. A plane-wave cutoff energy of 500 eV was deemed appropriate for these calculations. Brillouin zones of the 1×1×2 supercell of $Fe_3GaTe_2$-$O_x$ were sampled using a 12×12×2 k-point mesh. To ascertain the system energies for the antiferromagnetic (AFM) and ferromagnetic (FM) states, a two-stage methodology was implemented. Initially, structural optimizations were conducted employing Gaussian smearing, ensuring that the forces converged to values below 0.001 eV/Å. Following this, spin-orbit coupling was integrated into the calculations, and the system's total energy was determined as a function of the spin configuration, as elucidated in **Figure S5**. In the final stage, the EDIFF convergence threshold was set to $10^{-8}$ eV, and the tetrahedron method, complemented by Blöchl corrections, was applied to achieve a precise determination of the total energy.

The exchange interactions between atoms were obtained through energy mapping method[6,7]. To improve the computational accuracy, a 2×2×2 supercell was used, and calculations were performed for four different spin states. The nearest-neighbor exchange coupling $J_{11}$ between $Fe_1$ and $Fe_1$ and the next-nearest-neighbor exchange coupling $J_{12}$ between $Fe_1$ and $Fe_2$ were obtained. Considering that the exchange coupling beyond the next-nearest neighbor is too weak, we chose to neglect it. The results showed that both exchange interactions remained ferromagnetic before and after oxidation. Before oxidation, $J_{11} \approx -0.247eV$ and $J_{12} \approx -0.372eV$ ,while after complete oxidation, $J_{11} \approx -0.016eV$ and $J_{12} \approx -0.0031eV$. This demonstrates that the antiferromagnetic coupling does not originate from intralayer oxidation but rather from interlayer interactions. Additionally, the frequency-dependent dielectric function of Fe3GaTe2 and O-Fe3GaTe2 is based on the independent-particle approximation8, with the wavefunction derived from previous calculations.

In our DFT calculations, we adopted specific supercell models, assuming a uniformly oxidized structure for $Fe_3GaTe_2$ flakes. However, in real experimental conditions, oxidation might not be strictly uniform due to local variations in surface reactivity, defects, and environmental factors. This nonuniformity can lead to slight local variations in oxygen coverage, potentially resulting in variations in the strength of interfacial spin pinning across different regions of the sample. While this limitation does not invalidate our conclusions regarding the overall exchange bias behavior, it is important to acknowledge that local inhomogeneity may contribute to minor quantitative differences observed experimentally.

Based on the interlayer coupling strength obtained from DFT calculations as listed in Supplementary Table 1, the magnetic field which convert the antiferromagnets to ferromagnets can be determined using the following equation:

$$H_s = \frac{2J_{IEC}}{\mu_0 M_s t_{FM}} \qquad \text{(Eq. S1)}$$

where $\mu_0$ is the vacuum permeability $4\pi \times 10^{-7}\mathrm{N/A^2}$, $t_{FM}$ is the thickness of the ferromagnetic layer, and $M_s$ is the saturation magnetization, defined as the total magnetic moment of all magnetic atoms in a unit cell divided by the unit cell volume. $J_{IEC}$ represents the energy difference between the ferromagnetic and antiferromagnetic states of the unit cell.

Our calculations show that fully magnetizing the antiferromagnetic state of the completely oxidized O-$Fe_3GaTe_2$ in one direction requires a magnetic field of approximately 443.7 T. This exceptionally strong antiferromagnetic coupling prevents the observation of antiferromagnetic spin flip steps even under an applied field of 6 T. However, this value represents an idealized interface; in reality, the complex interface structure in O- $Fe_3GaTe_2$ reduces the required field. For example, in the typical Ruderman-Kittel-Kasuya-Yosida (RKKY) coupling effect, the

experimentally observed antiferromagnetic coupling strength is often significantly smaller than the theoretical predicted value[8,9].

DFT calculations further indicate that interlayer coupling is antiferromagnetic only when both layers are oxidized. At the interface between fully oxidized O-$Fe_3GaTe_2$ and $Fe_3GaTe_2$, the coupling is ferromagnetic. Since the partial oxidation layer is a transition region at the interface between the fully oxidized layer and the pristine layer, the competition between ferromagnetic and antiferromagnetic interactions at this interface leads to a complex magnetic domain structure. Although a setting field of 2 T–4 T is insufficient to magnetize antiferromagnetically coupled O-$Fe_3GaTe_2$, it is strong enough to influence the direction and size of complex magnetic domains at the interface, thereby determining the direction of the exchange bias[10].

**Supplementary Note S3. Penetration depth estimation**

The penetration depth $\delta_p$ is defined to describe the depth at which the power density of an electromagnetic wave is reduced to its 1/*e*, which can be expressed in the following form[11]:

$$\delta_p = \frac{1}{2}\left\{\frac{\lambda}{2\pi}\left[\frac{2}{\varepsilon_r' \cdot \left(\sqrt{1+\tan^2\left(\varepsilon_r''/\varepsilon_r'\right)}-1\right)}\right]^{\frac{1}{2}}\right\} \qquad \text{(Eq. S2)}$$

where $\varepsilon_r'$ and $\varepsilon_r''$ is the real and imaginary parts of complex permittivity, respectively. For the 532 nm laser, the estimated $\delta_p$ of the fully oxidized $Fe_3GaTe_2$ is about 75 nm and the estimated $\delta_p$ of the $Fe_3GaTe_2$ is about 31 nm. For the 633 nm laser, the estimated $\delta_p$ of the fully oxidized $Fe_3GaTe_2$ is about 23 nm and the estimated $\delta_p$ of the $Fe_3GaTe_2$ is about 93 nm.

**References**


1 Patil, C. *et al.* Highly accurate, reliable, and non-contaminating two-dimensional material transfer system. *Applied Physics Reviews* **9** (2022). https://doi.org/10.1063/5.0071799

2 Bie, Y.-Q., Zong, A., Wang, X., Jarillo-Herrero, P. & Gedik, N. A versatile sample fabrication method for ultrafast electron diffraction. *Ultramicroscopy* **230**, 113389 (2021). https://doi.org/https://doi.org/10.1016/j.ultramic.2021.113389

3 Kresse, G. & Hafner, J. Ab initio molecular dynamics for open-shell transition metals. *Physical Review B* **48**, 13115 (1993).

4 Kresse, G. & Furthmüller, J. Efficient iterative schemes for ab initio total-energy calculations using a plane-wave basis set. *Physical review B* **54**, 11169 (1996).

5 Perdew, J. P., Burke, K. & Ernzerhof, M. Generalized gradient approximation made simple. *Physical review letters* **77**, 3865 (1996).

6 Xiang, H. J., Kan, E. J., Wei, S.-H., Whangbo, M. H. & Gong, X. G. Predicting the spin-lattice order of frustrated systems from first principles. *Physical Review B* **84** (2011). https://doi.org/10.1103/PhysRevB.84.224429

7 Yang, J. H. *et al.* Strong Dzyaloshinskii-Moriya interaction and origin of ferroelectricity in Cu2OSeO3. *Phys Rev Lett* **109**, 107203 (2012). https://doi.org/10.1103/PhysRevLett.109.107203

8 Liu, X., Ishio, S. & Ma, H. Study of magnetization reversal process in FeCo/Ru/FeCo exchange coupled synthetic antiferromagnetic multilayers. *Journal of Nanomaterials* **2015** (2015).

9 Yang, Q. *et al.* Ionic liquid gating control of RKKY interaction in FeCoB/Ru/FeCoB and (Pt/Co)2/Ru/(Co/Pt)2 multilayers. *Nat. Commun.* **9**, 991 (2018). https://doi.org/10.1038/s41467-018-03356-z

10 Ohldag, H. *et al.* Correlation between Exchange Bias and Pinned Interfacial Spins. *Physical Review Letters* **91**, 017203 (2003). https://doi.org/10.1103/PhysRevLett.91.017203

11 Fluhrer, A. *et al.* Remote Sensing of Complex Permittivity and Penetration Depth of Soils Using P-Band SAR Polarimetry. *Remote Sensing* **14**, 2755 (2022).